Spin-polarized parametric pumping: Theory and numerical results

Junling Wu,[1] Baigeng Wang,[1] and Jian Wang[1,2,*]
[1]*Department of Physics, The University of Hong Kong, Pokfulam Road, Hong Kong, China*
[2]*Institute of Solid State Physics, Chinese Academy of Sciences, Hefei, Anhui, China*
(Received 29 April 2002; revised manuscript received 12 July 2002; published 27 November 2002)

We have extended the previous parametric electron pumping theory to include the spin-polarized pumping effect. Specifically, we consider a parametric pump consisting of a nonmagnetic system with two ferromagnetic leads whose magnetic moments orient at an angle θ with respect to each other. In our theory, the leads can be maintained at different chemical potentials. As a result, the current is driven due to both the external bias and the pumping potentials. When both θ and the external bias are zero, our theory recovers the known theory. In particular, two cases are considered: (i) in the adiabatic regime, we have derived the pumped current for an arbitrary pumping amplitude and external bias and (ii) at finite frequency, the system is away from equilibrium, and we have derived the pumped current up to quadratic order in pumping amplitude. From our numerical results we found that the pumped current can be modulated by the angle θ, showing interesting spin-valve effects.

DOI: 10.1103/PhysRevB.66.205327 PACS number(s): 73.23.Ad, 73.40.Gk, 72.10.Bg

I. INTRODUCTION

Recently, there has been considerable interest in parametric pumping.[1–29] The parametric pump is facilitated by cyclic variations of pumping potentials inside the scattering system and has been realized experimentally by Switkes *et al.*[3] On the theoretical side, much progress has been made towards understanding various features related to the parametric pump. This includes quantization of the pumped charge,[2,9,20,25] the influence of discrete spatial symmetries and magnetic field,[5,7] the rectification of displacement current,[10] as well as inelastic scattering[11] to the pumped current. The concept of an optimal pump has been proposed with the lower bound for the dissipation derived.[12] Within the formalism of time-dependent scattering matrix theory, the heat current and shot noise in the pumping process[17,23,24,27] has also been discussed. Recently, the original adiabatic pumping theory has been extended to account for the effect due to finite frequency,[14,19] Andreev reflection in the presence of superconducting leads,[13,28] and strong electron interaction in the Kondo regime.[26] This gives us more physical insight into parametric pumping. For instance, the experimentally observed anomaly of pumped current at $\phi=0$ and $\phi=\pi$ can be explained using finite frequency theory[19] as due to the quantum interference of different photon-assisted processes. When a superconducting lead is present, the interference between the direct reflection and multiple Andreev reflections gives rise to an enhancement of pumped current which is four times that of the normal system.[13] It will be interesting to further extend the parametric theory to the case where the ferromagnetic leads are present. With the theory extended, much different physics is foreseen[30] which may lead to operational paradigms for future spintronic devices.[31] In this paper, we have extended the previous parametric electron pumping theory to include the spin-polarized pumping effect. Specifically, we consider a parametric pump consisting of a nonmagnetic system with two ferromagnetic leads whose magnetic moments orient at an angle θ with respect to each other. Our theory is based on a nonequilibrium Green's-function approach and focused on current perpendicular to plane geometry. The parametric pump generates current at zero external bias. It would be interesting to see the interplay of the role played by the pumping potential and external bias if the leads are maintained at different chemical potentials.[22] Hence in our theory, the external bias is also included. In the adiabatic regime, the pumped current is proportional to pumping frequency. In this regime, we have derived the parametric pumping theory for finite pumping amplitude. At the finite pumping frequency, the system is away from equilibrium, and we have performed perturbation up to the second order in pumping amplitude and obtained the pumped current at finite frequencies. Our theory allows one to study the pumped current for a variety of parameters, such as the pumping amplitude, pumping frequency, phase difference between two pumping potentials, the angular dependence between the magnetization of two leads, as well as the external bias. We have applied our theory to a tunneling magnetoresistance (TMR) junction.[32] Due to the reported room-temperature operation of TMR, the fundamental principle and transport properties of TMR devices have attracted increasing attention.[33] From our numerical results we found that the pumped current can be modulated by the angle θ showing interesting spin-valve effects. The paper is organized as follows. In Sec. II, we derive the general theory of a parametric pump in the presence of ferromagnetic leads. The numerical results and summary are presented in Sec. III.

II. THEORY

The system we examine consists of a nonmagnetic system connected by two ferromagnetic electrodes to the reservoir. The magnetic moment **M** of the left electrode is pointing in the z direction, the electric current is flowing in the y direction, while the moment of the right electrode is at an angle θ to the z axis in the x-z plane (see the inset of Fig. 1 for a schematic picture). The Hamiltonian of the system is of the following form:

$$H=H_L+H_R+H_0+V_p+H_T, \tag{1}$$

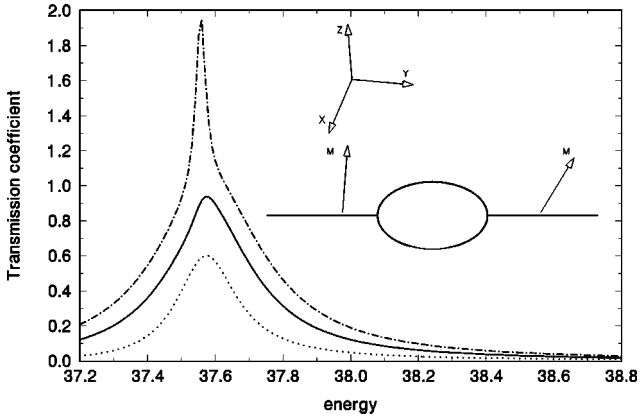

FIG. 1. The transmission coefficient as a function of Fermi energy at different angles θ between the magnetizations of two leads: $\theta=0$ (dashed line), $\theta=\pi/2$ (solid line), and $\theta=\pi$ (dotted line). Inset: schematic picture of the system.

where H_L and H_R describe the left and right electrodes,

$$H_L=\sum_{k\sigma}(\epsilon_{kL}+\sigma M)c^{\dagger}_{kL\sigma}c_{kL\sigma}, \tag{2}$$

$$H_R=\sum_{k\sigma}\Big[(\epsilon_{kR}+\sigma M\cos\theta)c^{\dagger}_{kR\sigma}c_{kR\sigma} + \sum_{k\sigma} M\sin\theta[c^{\dagger}_{kR\sigma}c_{kR\bar{\sigma}}]. \tag{3}$$

In Eq. (1), H_0 describes the nonmagnetic (NM) scattering region,

$$H_0=\sum_{n\sigma}\epsilon_n d^{\dagger}_{n\sigma}d_{n\sigma}. \tag{4}$$

V_p is the time-dependent pumping potential and H_T describes the coupling between electrodes and the NM scattering region with hopping matrix $T_{k\alpha n}$. To simplify the analysis, we assume the hopping matrix to be independent of spin index, hence

$$H_T=\sum_{k\alpha n\sigma}[T_{k\alpha n}c^{\dagger}_{k\alpha\sigma}d_{n\sigma}+\text{c.c.}]. \tag{5}$$

In these expressions $\epsilon_{k\alpha}=\epsilon^0_k+qV_\alpha$ with $\alpha=L,R$; $c^{\dagger}_{k\alpha\sigma}$ (with $\sigma=\uparrow,\downarrow$ or ±1, and $\bar{\sigma}=-\sigma$) is the creation operator of electrons with spin index σ inside the α electrode. Similarly $d^{\dagger}_{n\sigma}$ is the creation operator of electrons with spin σ at energy level n for the NM scattering region. In writing Eqs. (2) and (3), we have made a simplification that the value of the molecular field M is the same for the two electrodes, thus the spin-valve effect is obtained[32] by varying the angle θ. Essentially, M mimics the difference of the density of states between spin-up and -down electrons[32] in the electrodes. In this paper, we only consider the single electron behavior. The charge quantization is not considered so that our system is not in the Coulomb blockade regime. In addition, for the nonmagnetic regions in which we are interested, the Kondo effect can be neglected.

To proceed, we first apply the following Bogoliubov transformation[34] to diagonalize the Hamiltonian of the right electrode,[35]

$$c_{kR\sigma}\rightarrow\cos(\theta/2)C_{kR\sigma}-\sigma\sin(\theta/2)C_{kR\bar{\sigma}}, \tag{6}$$

$$c^{+}_{kR\sigma}\rightarrow\cos(\theta/2)C^{+}_{kR\sigma}-\sigma\sin(\theta/2)C^{+}_{kR\bar{\sigma}}, \tag{7}$$

from which we obtain the effective Hamiltonian

$$H_R=\sum_{k\sigma}[(\epsilon_{kR}+\sigma M)C^{\dagger}_{kR\sigma}C_{kR\sigma}], \tag{8}$$

$$H_T=\sum_{kn\sigma}\Big[T_{kLn}c^{\dagger}_{kL\sigma}d_{n\sigma}+T_{kRn}\Big(\cos\frac{\theta}{2}C^{\dagger}_{kR\sigma} - \sigma\sin\frac{\theta}{2}C^{\dagger}_{kR\bar{\sigma}}\Big)d_{n\sigma}+\text{c.c.}\Big]. \tag{9}$$

In the following subsections, we will consider two cases: (i) parametric pumping in the low-frequency limit with finite pumping amplitude and (ii) pumping in the weak pumping limit with finite pumping frequency.

A. Pumping in the low-frequency limit

In this subsection, we examine the pumping current at the low-frequency limit while maintaining the pumping amplitude finite. In this limit, the system is nearly in equilibrium and we will use the equilibrium Green's function[36–38] to characterize the pumping process. Using the distribution function, the total charge in the system during the pumping is given by

$$Q(x,t)=-iq\int(dE/2\pi)[\mathbf{G}^{<}(E,\{V(t)\})]_{xx}, \tag{10}$$

where $\mathbf{G}^{<}$ is the lesser Green's function in real space, x labels the position, and $\{V(t)\}$ describes a set of external parameters which facilitates the pumping process. Within a Hartree approximation, $\mathbf{G}^{<}$ is related to the retarded and advanced Green's functions $\mathbf{G}^r$ and $\mathbf{G}^a$,

$$\mathbf{G}^{<}(E,\{V\})=\mathbf{G}^r(E,\{V\})i\sum_\alpha\mathbf{\Gamma}_\alpha f_\alpha(E)\mathbf{G}^a(E,\{V\}), \tag{11}$$

where $f_\alpha(E)=f(E-qV_\alpha)$. In the low-frequency limit, the retarded Green's function in real space is given by

$$\mathbf{G}^r(E,\{X\})=\frac{1}{E-H_0-\mathbf{V}_p-\mathbf{\Sigma}^r}, \tag{12}$$

where $\mathbf{\Sigma}^r\equiv\Sigma_\alpha\mathbf{\Sigma}^r_\alpha$ is the self-energy, and $\mathbf{\Gamma}_\alpha=-2\,\text{Im}[\mathbf{\Sigma}^r_\alpha]$ is the linewidth function. In the above equations, $\mathbf{G}^{r,a,<}$ denotes a 2×2 matrix with matrix elements $G^{r,a<}_{\sigma,\sigma'}$ and $\sigma=\uparrow,\uparrow$. $\mathbf{V}_p=V_p\mathbf{I}$ where $\mathbf{I}$ is a 2×2 unit matrix in the spin space. In a real-space representation, V_p is a diagonal matrix

describing the variation of the potential landscape due to the external pumping parameter V. The self-energies are given by[35]

$$\mathbf{\Sigma}^r_\alpha(E)=\hat{R}_\alpha\begin{pmatrix}\Sigma^r_{\alpha\uparrow} & 0\\ 0 & \Sigma^r_{\alpha\downarrow}\end{pmatrix}\hat{R}^\dagger_\alpha \tag{13}$$

and

$$\mathbf{\Sigma}^<_\alpha(E)=if_\alpha\hat{R}_\alpha\begin{pmatrix}\Gamma^0_{\alpha\uparrow} & 0\\ 0 & \Gamma^0_{\alpha\downarrow}\end{pmatrix}\hat{R}^\dagger_\alpha \tag{14}$$

with the rotational matrix $\hat{R}_\alpha$ for electrode α defined as

$$\hat{R}=\begin{pmatrix}\cos\theta_\alpha/2 & \sin\theta_\alpha/2\\ -\sin\theta_\alpha/2 & \cos\theta_\alpha/2\end{pmatrix}. \tag{15}$$

Here angle θ_α is defined as $\theta_L=0$ and $\theta_R=\theta$,$\Sigma^r_{\alpha\sigma}$ is given by

$$\Sigma^r_{\alpha\sigma mn}=\sum_k\frac{T^*_{k\alpha m}T_{k\alpha n}}{E-\epsilon^0_{k\alpha\sigma}+i\delta}, \tag{16}$$

and $\Gamma^0_{\alpha\sigma}=-2\,\mathrm{Im}(\Sigma^r_{\alpha\sigma})$ is the linewidth function when $\theta=0$.

In order for a parametric electron pump to function at low frequency, we need simultaneous variation of two or more system parameters controlled by gate voltages: $V_i(t)=V_{i0}+V_{ip}\cos(\omega t+\phi_i)$. Hence, in our case, the potential due to the gates can be written as $V_p=\Sigma_i V_i\mathbf{\Delta}_i$, where $\mathbf{\Delta}_i$ is the potential profile due to each pumping potential. For simplicity we assume a constant gate potential such that $(\mathbf{\Delta}_1)_{xx}$ is one for x in the first gate region and zero otherwise. If the time variation of these parameters is slow, i.e., for $V(t)=V_0+\delta V\cos(\omega t)$, then the charge of the system coming from all contacts due to the infinitesimal change of the system parameter ($\delta V\to 0$) is

$$dQ_p(t)=\sum_i\partial_{V_i}\mathrm{Tr}[Q(x,t)]\,\delta V_i(t). \tag{17}$$

It is easily seen that the total charge in the system in a period is zero which is required for the charge conservation. To calculate the pumped current, we have to find the charge $dQ_{p\alpha}$ passing through contact α due to the change of the system parameters. Using the Dyson equation $\partial_{V_i}\mathbf{G}^r=\mathbf{G}^r\Delta_i\mathbf{G}^r$, the above equation becomes

$$\begin{aligned}dQ_p(t)&=q\sum_j\int\frac{dE}{2\pi}\sum_\beta\mathrm{Tr}[\mathbf{G}^r\mathbf{\Delta}_j\mathbf{G}^r\mathbf{\Gamma}_\beta\mathbf{G}^a\\&\quad+\mathbf{G}^r\mathbf{\Gamma}_\beta\mathbf{G}^a\mathbf{\Delta}_j\mathbf{G}^a]f_\beta(E)\,\delta V_j(t)\\&=-q\int\frac{dE}{2\pi}\sum_j\sum_\beta f_\beta\mathrm{Tr}(\partial_E[\mathbf{G}^a\mathbf{\Gamma}_\beta\mathbf{G}^r\mathbf{\Delta}_j])\,\delta V_j(t),\end{aligned}$$

where the wideband limit has been taken. Integrating by part, we obtain

$$dQ_p(t)=q\int dE\sum_\beta(\partial_E f_\beta)\sum_j\frac{dN_\beta}{dV_j}\delta V_j(t), \tag{18}$$

where we have used the injectivity[40]

$$\frac{dN_\beta}{dV_j}=\frac{1}{2\pi}\mathrm{Tr}[\mathbf{G}^a\mathbf{\Gamma}_\beta\mathbf{G}^r\mathbf{\Delta}_j]. \tag{19}$$

Using the partial density of states $dN_{\alpha\beta}/dV_j$ defined as[41]

$$\begin{aligned}\frac{dN_{\alpha\beta}}{dV_j}&=\frac{1}{4\pi}\mathrm{Tr}[\mathbf{G}^r\mathbf{\Gamma}_\alpha\mathbf{G}^r\Delta_j+\mathrm{c.c.}]\,\delta_{\alpha\beta}\\&\quad+\frac{1}{4\pi}\mathrm{Tr}[i\mathbf{G}^r\mathbf{\Gamma}_\alpha\mathbf{G}^a\mathbf{\Gamma}_\beta\mathbf{G}^r\Delta_j+\mathrm{c.c.}]\end{aligned} \tag{20}$$

with $\Sigma_\alpha dN_{\alpha\beta}/dV_j=dN_\beta/dV_j$, we obtain

$$dQ_{p\alpha}(t)=-q\int dE\sum_\beta(-\partial_E f_\beta)\sum_j\frac{dN_{\alpha\beta}}{dV_j}\delta V_j(t). \tag{21}$$

If we include the charge passing through contact α due the external bias, then

$$\begin{aligned}dQ_\alpha(t)&=-q\int dE\sum_\beta(-\partial_E f_\beta)\sum_j\frac{dN_{\alpha\beta}}{dV_j}\frac{dV_j(t)}{dt}dt\\&\quad-q\int dE\sum_\beta\mathrm{Tr}[\mathbf{\Gamma}_\alpha\mathbf{G}^r\mathbf{\Gamma}_\beta\mathbf{G}^a](f_\alpha-f_\beta)dt.\end{aligned} \tag{22}$$

Furthermore, the total current flowing through contact α due to both the variation of parameters V_j and external bias, in one period, is given by

$$J_\alpha=\frac{1}{\tau}\int_0^\tau dt\,dQ_\alpha/dt, \tag{23}$$

where $\tau=2\pi/\omega$ is the period of cyclic variation. If there are two pumping parameters, Eq. (23) can be written as when $\alpha=1$,

$$\begin{aligned}J^{(1)}_1&=\frac{q}{2\tau}\int dt\int dE\;\partial_E(f_1-f_2)\sum_j\left[\frac{dN_{11}}{dV_j}\frac{dV_j(t)}{dt}\right.\\&\quad\left.-\frac{dN_{12}}{dV_j}\frac{dV_j(t)}{dt}\right]dt\\&\quad-\frac{q}{\tau}\int dt\int dE\,\mathrm{Tr}[\mathbf{\Gamma}_1\mathbf{G}^r\mathbf{\Gamma}_2\mathbf{G}^a](f_1-f_2)\end{aligned} \tag{24}$$

and

$$\begin{aligned}J^{(2)}_1&=\frac{q}{2\tau}\int dt\int dE\,\partial_E(f_1+f_2)\sum_j\left[\frac{dN_{11}}{dV_j}\frac{dV_j(t)}{dt}\right.\\&\quad\left.+\frac{dN_{12}}{dV_j}\frac{dV_j(t)}{dt}\right]dt,\end{aligned} \tag{25}$$

where $J_1=J^{(1)}_1+J^{(2)}_2$. In Ref. 22, $J^{(1)}_1$ has been identified as the current due to the external bias and $J^{(2)}$ as pumping current. For $\theta=0,\pi$, all of the 2×2 matrix is diagonal. In

this case, it is easy to show that Eq. (23) agrees with the result of Ref. 22. If the external bias is zero, Eq. (23) reduces to the familiar formula[1] when there are two pumping potentials,

$$J_\alpha = \frac{q\omega}{2\pi}\int_0^\tau dt\left[\frac{dN_\alpha}{dX_1}\frac{dX_1}{dt}+\frac{dN_\alpha}{dX_2}\frac{dX_2}{dt}\right]. \tag{26}$$

B. Finite frequency pumping in the weak pumping limit

In this subsection, we will calculate the pumping current at finite frequency. The Keldysh nonequilibrium Green's-function approach used here is in the standard tight-binding representation.[36] We could not use the momentum space version because the time-dependent perturbation (pumping potential) inside the scattering region is position dependent. Hence it is most suitable to use a tight-binding real-space technique. In contrast, in previous investigations[39] on photon-assisted processes the time-dependent potential is uniform throughout the dot and therefore a momentum space method is easier to apply.

Assuming the time-dependent perturbations located at the different sites, $j=i_0$, j_0, and k_0, etc. with

$$V_j(t) = V_j\cos(\omega t+\phi_j). \tag{27}$$

When there is no interaction between electrons in the ideal leads L and R, the standard nonequilibrium Green's-function theory gives the following expression for the time-dependent current,[37]

$$J_\alpha(t) = -q\int_{-\infty}^{t} dt_1 \mathrm{Tr}[\mathbf{G}^r(t,t_1)\mathbf{\Sigma}_\alpha^<(t_1,t)+\mathbf{G}^<(t,t_1)\mathbf{\Sigma}_\alpha^a(t_1,t) + \text{c.c.}] \tag{28}$$

and a transmission coefficient

$$T(E) = \mathrm{Tr}[\mathbf{\Gamma}_L^r(E)\mathbf{G}^r(E)\mathbf{\Gamma}_R^r(E)\mathbf{G}^a(E)], \tag{29}$$

where the scattering Green's functions and self-energy are defined in the usual manner:

$$\mathbf{G}^{r,a}_{ij\sigma\sigma'}(t_1,t_2) = \mp i\,\theta(\pm t_1 \mp t_2)\langle\{d_{i,\sigma}(t_1),d^+_{j,\sigma'}(t_2)\}\rangle, \tag{30}$$

$$\mathbf{G}^<_{ij,\sigma,\sigma'}(t_1,t_2) = i\langle d^+_{j,\sigma'}(t_2)d_{i,\sigma,}(t_1)\rangle, \tag{31}$$

$$\mathbf{\Sigma}^{r,a,<}_{\alpha ij}(t_1,t_2) = \sum_k T^*_{\alpha ki}T_{\alpha kj}\mathbf{g}^{r,a,<}_\alpha(t_1,t_2). \tag{32}$$

The average current $J_L(t)$ from the left lead can be written as

$$\langle J_L(t)\rangle = -\frac{q}{\tau}\int_0^\tau dt\int_{-\infty}^{t} dt_1 \mathrm{Tr}[\mathbf{G}^r_{11}(t,t_1)\mathbf{\Sigma}_L^<(t_1,t) + \mathbf{G}^<_{11}(t,t_1)\mathbf{\Sigma}_L^a(t_1,t) + \text{c.c.}]. \tag{33}$$

In the absence of pumping, the retarded Green's function is defined in terms of the Hamiltonian H_0,

$$\mathbf{G}^{0r}(E) = \frac{1}{E-H_0-\mathbf{\Sigma}^r} \tag{34}$$

and $\mathbf{G}^{0<}$ is related to the retarded and advanced Green's functions $\mathbf{G}^{0r}$ and $\mathbf{G}^{0a}$ by

$$\mathbf{G}^{0<}(E) = \mathbf{G}^{0r}(E)\mathbf{\Sigma}^<(E)\mathbf{G}^{0a}(E). \tag{35}$$

Now we make use of the time-dependent pumping potentials $V_j(t)$ as the perturbations to calculate all kinds of Green's functions up to the second order, and corresponding average current.

First, we calculate the current corresponding to the term $\mathbf{G}^r_{11}(t,t_1)\mathbf{\Sigma}_L^<(t_1,t)$ in Eq. (33). The Dyson equation for $\mathbf{G}^r_{11}(t,t_1)$ gives the second-order contribution

$$\begin{aligned}\mathbf{G}^{(2)r}_{11}(t,t_1) &= \sum_{jk}\int\int dxdy\,\mathbf{G}^{0r}_{1j}(t-x)\mathbf{V}_j(x)\mathbf{G}^{0r}_{jk}(x-y)\\ &\quad\times\mathbf{V}_k(y)\mathbf{G}^{0r}_{k1}(y-t_1)\\ &\equiv \sum_{jk}\mathbf{G}^{0r}_{1j}\mathbf{V}_j\mathbf{G}^{0r}_{jk}\mathbf{V}_k\mathbf{G}^{0r}_{k1}.\end{aligned} \tag{36}$$

Substituting Eq. (36) into Eq. (33) and completing the integration over time x,y,t_1,t, it is not difficult to calculate the average current $\langle J_{L1}\rangle$ due to the first term in Eq. (33) (see the Appendix for details),

$$\langle J_{L1}(t)\rangle = -\sum_{jk}\frac{qV_jV_k}{4}\int\frac{dE}{2\pi}\mathrm{Tr}\{\mathbf{\Sigma}_L^<\mathbf{G}^{0r}_{1j}[\mathbf{G}^{0r}_{jk}(E_-)e^{i\Delta_{kj}} + \mathbf{G}^{0r}_{jk}(E_+)e^{-i\Delta_{kj}}]\mathbf{G}^{0r}_{k1}\}, \tag{37}$$

where $\Delta_{kj}=\phi_k-\phi_j$ is the phase difference, $E_\pm = E\pm\omega$, and $G^{r,a,<}\equiv G^{r,a,<}(E)$.

Now we calculate the second term $\mathbf{G}^<_{11}(t,t_1)\mathbf{\Sigma}^a_L(t_1,t)$ in Eq. (33). Using the Keldysh equation, $\mathbf{G}^<=\mathbf{G}^r\mathbf{\Sigma}^<\mathbf{G}^a$, we have

$$\mathbf{G}^<_{jk} = \mathbf{G}^r_{j1}\mathbf{\Sigma}_L^<\mathbf{G}^a_{1k}+\mathbf{G}^r_{jN}\mathbf{\Sigma}_R^<\mathbf{G}^a_{Nk}, \tag{38}$$

where $\mathbf{\Sigma}^<_\alpha = i\mathbf{\Gamma}_\alpha f_\alpha$. Expanding $G^{r,a}$ up to the second order in pumping parameters, we obtain the second-order contribution from $\mathbf{G}^<_{11}$,

$$\begin{aligned}\mathbf{G}^{(2)<}_{11} &= \mathbf{G}^r_{11}\mathbf{\Sigma}_L^<\mathbf{G}^a_{11}+\mathbf{G}^r_{1N}\mathbf{\Sigma}_R^<\mathbf{G}^a_{N1}\\ &= \mathbf{G}^{(2)r}_{11}\mathbf{\Sigma}_L^<\mathbf{G}^{0a}_{11}+\mathbf{G}^{(1)r}_{11}\mathbf{\Sigma}_L^<\mathbf{G}^{(1)a}_{11}+\mathbf{G}^{0r}_{11}\mathbf{\Sigma}_L^<\mathbf{G}^{(2)a}_{11}\\ &\quad+\mathbf{G}^{(2)r}_{1N}\mathbf{\Sigma}_R^<\mathbf{G}^{0a}_{N1}+\mathbf{G}^{(1)r}_{1N}\mathbf{\Sigma}_R^<\mathbf{G}^{(1)a}_{N1}+\mathbf{G}^{0r}_{1N}\mathbf{\Sigma}_R^<\mathbf{G}^{(2)a}_{N1}\\ &= \sum_{jk}[\mathbf{G}^{0r}_{1j}\mathbf{V}_j\mathbf{G}^{0r}_{jk}\mathbf{V}_k\mathbf{G}^{0<}_{k1}+\mathbf{G}^{0r}_{1j}\mathbf{V}_j\mathbf{G}^{0<}_{jk}\mathbf{V}_k\mathbf{G}^{0a}_{k1}\\ &\quad+\mathbf{G}^{0<}_{1j}\mathbf{V}_j\mathbf{G}^{0a}_{jk}\mathbf{V}_k\mathbf{G}^{0a}_{k1}]\\ &= g_2+g_3+g_4,\end{aligned} \tag{39}$$

where we have used Eq. (38) to simplify the expression. Plugging Eq. (39) into Eq. (33) and after some algebra, we have the following three expressions corresponding to each term in Eq. (39),

$$\langle J_{L2}\rangle = \text{the term corresponding to} g_2 \text{ in Eq. (39)}$$
$$= -\sum_{jk}\frac{qV_jV_k}{4}\int\frac{dE}{2\pi}\mathrm{Tr}\{\mathbf{\Sigma}_L^a\mathbf{G}_{1j}^{0r}[\mathbf{G}_{jk}^{0r}(E_-)e^{i\Delta_{kj}} + e^{-i\Delta_{kj}}\mathbf{G}_{jk}^{0r}(E_+)]\mathbf{G}_{k1}^{0<}\}, \quad (40)$$

$$\langle J_{L3}\rangle = -\sum_{jk}\frac{qV_jV_k}{4}\int\frac{dE}{2\pi}\mathrm{Tr}\{\mathbf{\Sigma}_L^a\mathbf{G}_{1j}^{0r}[\mathbf{G}_{jk}^{0<}(E_-)e^{i\Delta_{kj}} + e^{-i\Delta_{kj}}\mathbf{G}_{jk}^{0<}(E_+)]\mathbf{G}_{k1}^{0a}\}, \quad (41)$$

$$\langle J_{L4}\rangle = -\sum_{jk}\frac{qV_jV_k}{4}\int\frac{dE}{2\pi}\mathrm{Tr}\{\mathbf{\Sigma}_L^a\mathbf{G}_{1j}^{0<}[\mathbf{G}_{jk}^{0a}(E_-)e^{i\Delta_{kj}} + e^{-i\Delta_{kj}}\mathbf{G}_{jk}^{0a}(E_+)]\mathbf{G}_{k1}^{0a}\}. \quad (42)$$

The final pumped current is the sum of Eqs. (37), (40)–(42), and their complex conjugates, in addition to the current directly due to the external bias [see second term of Eq. (24)]. If the external bias is zero, the expression of the pumped current can be simplified significantly. Note that in the equilibrium, the lesser Green's function satisfies the fluctuation-dissipation theorem,

$$\mathbf{G}^{0<}(E) = -f(E)[\mathbf{G}^{0r}(E) - \mathbf{G}^{0a}(E)] \quad (43)$$

and

$$\mathbf{G}^{0<}(E_\pm) = -f(E_\pm)[\mathbf{G}^{0r}(E_\pm) - \mathbf{G}^{0a}(E_\pm)]. \quad (44)$$

Eqs. (37), (40), and (42)* lead to

$$-i\sum_{jk}\frac{qV_jV_k}{4}\int\frac{dE}{2\pi}\mathrm{Tr}\{\mathbf{\Gamma}_L\mathbf{G}_{1j}^{0r}f(E)[\mathbf{G}_{jk}^{0r}(E_-)e^{i\Delta_{kj}} + e^{-i\Delta_{kj}}\mathbf{G}_{kj}^{0r}(E_+)]\mathbf{G}_{k1}^{0a}\}, \quad (45)$$

while Eqs. (37), (40)*, and (42) give

$$i\sum_{jk}\frac{qV_jV_k}{4}\int\frac{dE}{2\pi}\mathrm{Tr}\{\mathbf{\Gamma}_L\mathbf{G}_{1j}^{0r}f(E)[\mathbf{G}_{jk}^{0a}(E_-)e^{i\Delta_{kj}} + e^{-i\Delta_{kj}}\mathbf{G}_{jk}^{0a}(E_+)]\mathbf{G}_{k1}^{0a}\}. \quad (46)$$

Furthermore, Eq. (41) plus the complex conjugate becomes

$$i\sum_{jk}\frac{qV_jV_k}{4}\int\frac{dE}{2\pi}\mathrm{Tr}(\mathbf{\Gamma}_L\mathbf{G}_{1j}^{0r}\{f_-[\mathbf{G}_{jk}^{0r}(E_-) - \mathbf{G}_{jk}^{0a}(E_-)]e^{i\Delta_{kj}} + e^{-i\Delta_{kj}}f_+[\mathbf{G}_{jk}^{0r}(E_+) - \mathbf{G}_{jk}^{0a}(E_+)]\}\mathbf{G}_{k1}^{0a}), \quad (47)$$

where $f_\pm = f(E_\pm)$.

Combining Eqs. (45)–(47), we finally obtain

$$J_L = i\sum_{jk}\frac{qV_jV_k}{4}\int\frac{dE}{2\pi}\mathrm{Tr}(\mathbf{\Gamma}_L\mathbf{G}_{1j}^{0r}\{(f_- - f)[\mathbf{G}_{jk}^{0r}(E_-) - \mathbf{G}_{jk}^{0a}(E_-)]e^{i\Delta_{kj}} + e^{-i\Delta_{kj}}(f_+ - f)[\mathbf{G}_{jk}^{0r}(E_+) - \mathbf{G}_{jk}^{0a}(E_+)]\}\mathbf{G}_{k1}^{0a}). \quad (48)$$

In the limit of small frequency, we expand Eq. (48) up to the first order in frequency and use the fact that

$$\mathbf{G}^{0r} - \mathbf{G}^{0a} = -i\mathbf{G}^{0r}\mathbf{\Gamma}\mathbf{G}^{0a} \quad (49)$$

and the Dyson equation

$$\mathbf{G}_{ji}^{0r}\mathbf{G}_{ik}^{0r} = \frac{\partial\mathbf{G}_{jk}^{0r}}{\partial\mathbf{V_i}}. \quad (50)$$

We obtain

$$J_L = \sum_{jk}\frac{q\omega V_jV_k\sin(\Delta_{kj})}{2}\int\frac{dE}{2\pi}\partial_E f(E)\mathrm{Tr}\{\mathbf{\Gamma}_L\mathbf{G}_{1j}^{0r}(E) \times[\mathbf{G}_{jk}^{0r}(E) - \mathbf{G}_{jk}^{0a}(E)]\mathbf{G}_{k1}^{0a}(E)\}$$
$$= -\sum_{jk}\frac{iq\omega V_jV_k\sin(\Delta_{jk})}{2}\int\frac{dE}{2\pi}\partial_E f(E) \times\mathrm{Tr}\left[\mathbf{\Gamma}_L\frac{\partial\mathbf{G}_{11}^{0r}}{\partial\mathbf{V}_j}\mathbf{\Gamma}_L\frac{\partial\mathbf{G}_{11}^{0a}}{\partial\mathbf{V}_k} + \mathbf{\Gamma}_L\frac{\partial\mathbf{G}_{12}^{0r}}{\partial\mathbf{V}_j}\mathbf{\Gamma}_R\frac{\partial\mathbf{G}_{21}^{0a}}{\partial\mathbf{V}_k}\right], \quad (51)$$

which is the same as Ref. 1 when $\theta = 0$.

III. RESULTS

We now apply our formula, Eqs. (24), (25), and (48), to a TMR junction. For current perpendicular to the plane geometry, the TMR junction can be modeled by a one-dimensional quantum structure with a double barrier potential $U(x) = X_1\delta(x+a) + X_2\delta(x-a)$ where $2a$ is the well width. For this system the Green's function $G(x,x')$ can be calculated exactly.[43] The adiabatic pump that we consider is operated by changing barrier heights adiabatically and periodically: $X_1 = V_0 + V_p\sin(\omega t)$ and $X_2 = V_0 + V_p\sin(\omega t + \phi)$. In the following, we will study zero-temperature behavior of the pumped current. In the calculation, we have chosen $M = 37.0$ and $V_0 = 79.2$. Finally the unit is set by $\hbar = 2m = 1$.[42]

We first study the pumped current with two pumping potentials in the adiabatic regime. Figure 1 depicts the transmission coefficient T versus Fermi energy at several angles θ between magnetizations of ferromagnetic leads. In general, all the transmission coefficients display the resonant feature. At $\theta = 0$ the resonance is much sharper. As expected, among different angles, T is the largest at $\theta = 0$ and smallest at $\theta = \pi$ with the ratio $T_{max}(0)/T_{max}(\pi) \sim 4$. This gives the usual spin-valve effect.[32] Figure 2 plots the pumped current versus Fermi energy at different angles θ. Here we have set the phase difference of two pumping potentials to be $\pi/2$. Similar to the transmission coefficient, we obtain the largest pumped current at $\theta = 0$ and the smallest current at $\theta = \pi$. We found that the ratio $I_{max}(0)/I_{max}(\pi)$ is about the same as that of the transmission coefficient (see also the left inset of

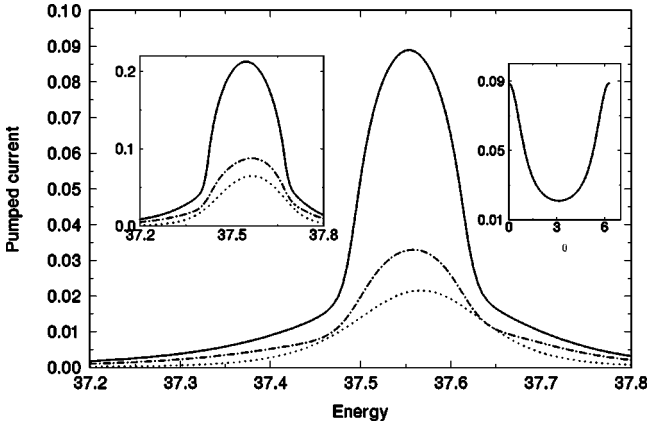

FIG. 2. The pumped current as a function of Fermi energy at different θ: $\theta=0$ (solid line), $\theta=\pi/2$ (dot-dashed line), and $\theta=\pi$ (dotted line). Other parameters are $\phi=\pi/2$ and $V_p=0.05V_0$. Left inset: the same as the main figure except $V_p=0.1V_0$. Right inset: the pumped current as a function of θ. Here $\phi=\pi/2$, $E_F=37.55$, and $V_p=0.05V_0$. For the unit for the pumped current, see Ref. 42.

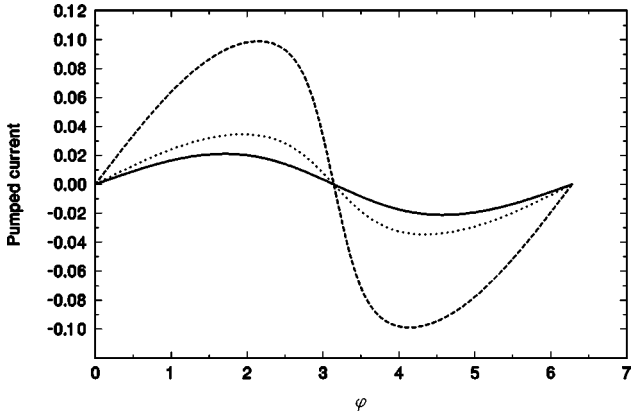

FIG. 3. The pumped current as a function of phase difference ϕ at different θ. $\theta=0$ (dashed line), $\theta=\pi/2$ (dotted line), and $\theta=\pi$ (solid line). Other parameters are $E_F=37.55$ and $V_p=0.05V_0$.

Fig. 2). This demonstrates the spin-valve effect for the pumped current. To understand this, we note that in the presence of the ferromagnetic leads, the electrons with spin up and down experience different potentials and hence generate different currents for different spin. Hence, because of the difference in density of states for spin-up and -down electrons, the pumped current is spin polarized. In addition as one varies the angle between magnetization in the ferromagnetic lead, the pumped current can be modulated by the angle θ. As the pumping amplitude doubles, the peak of pumped current is broadened and the maximum pumped current is nearly doubled (see the left inset of Fig. 2). This broadening is understandable since at large pumping amplitude the instantaneous resonant level oscillates with a large amplitude and hence can generate heat current in a broad range of energy. The doubling effect of the pumped current, as pumping amplitude doubles, persists for larger pumping amplitude. The physics may be different from that of Ref. 5. For an adiabatic pump, the pumped current is sensitive to the configuration of the system. After the random average over different configurations, Ref. 5 found that the pumped current scales as the square root of the pumping amplitude. For a chaotic system, Brouwer[10] found similar results. However, our system is not chaotic. It is in the ballistic regime and does not require the random average over a different configuration. However, since our pumping amplitude is not large enough, we cannot rule out that the range of our pumping amplitude is in the intermediate regime. The spin-valve effect of pumped current is illustrated in the right inset of Fig. 2 where the pumped current versus the angles θ is shown when the system is at resonance. We see that the pumped current is maximum at $\theta=0$ and decreases quickly as one increases θ from 0 to π. For larger pumping amplitude, we have similar behavior (not shown). In Fig. 3, we plot the pumped current, as a function of phase difference ϕ between two pumping potentials. We see that the pumped current is antisymmetric about the $\phi=\pi$. In the weak pumping regime, the dependence of pumped current as a function of the phase difference is sinusoidal.[1] In Fig. 3, the nonlinear behavior is clearly seen which deviates from the sinusoidal behavior at small pumping amplitude, indicating the onset of the strong pumping regime. We also notice that the peak of the pumped current shifts to the larger ϕ. In Fig. 4, we show the pumped current in the presence of external bias. In the calculation we assume that $V_L=-\omega V/2$ and $V_R=\omega V/2$ so that the external bias is against the pumped current when V is positive. Due to the external bias, the total pumped current (dashed line) decreases near resonant energy and reverses the direction at other energies. Now we turn to the case of finite frequency pumping. We first present our results (Fig. 5–Fig. 7) at small pumping frequency $\omega=0.002$. In Fig. 5 we plot the pumped current as a function of phase difference ϕ near the resonant energy. At $\theta=0$, the magnitude of pumped current is much larger than that at $\theta=\pi/2$ or π. This again demonstrates the spin-valve effect for the pumped current at finite frequency. We notice that at $\phi=0$ and $\phi=\pi$, the pumped current is nonzero, similar to the experimental anomaly observed experimentally for a nonmagnetic system.[3] The pumped current away from resonant energy is

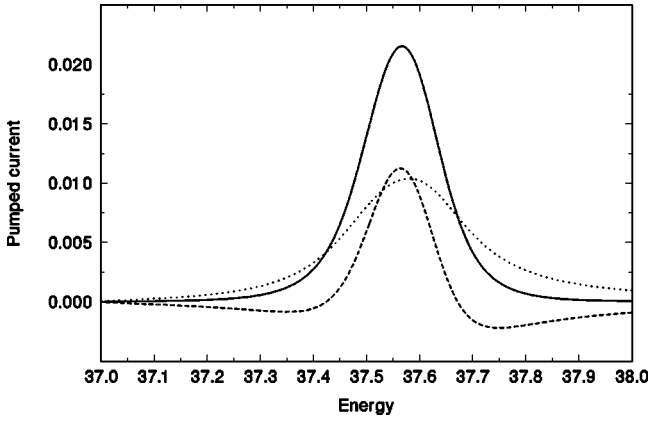

FIG. 4. The pumped current as a function of Fermi energy with an external bias $V_L-V_R=-0.02\omega$ at $\theta=\pi$. Solid line: pumped current, dotted line: current due to external bias, dashed line: total current. Here $\phi=\pi/2$ and $V_p=0.05V_0$. For $\theta=\pi/2$ and $\theta=0$ similar behavior is observed.

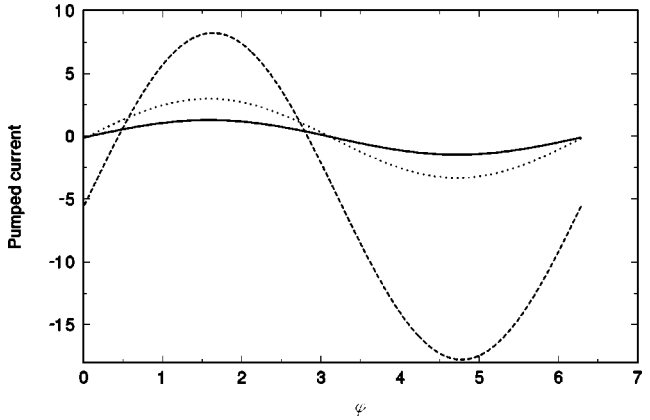

FIG. 5. The pumped current as a function of ϕ at finite frequency. Dashed line: $\theta=0$, dotted line: $\theta=\pi/2$, and solid line: $\theta=\pi$. Here $E_F=37.55$ and $\omega=0.002$.

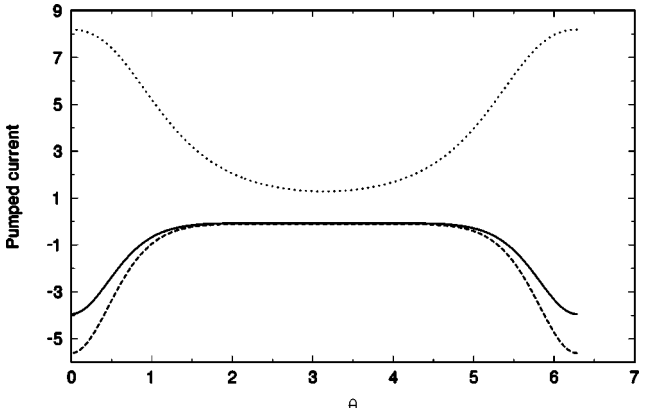

FIG. 7. The pumped current as a function of θ at finite frequency. Here dashed line: $\phi=0$, dotted line: $\phi=\pi/2$, and solid line: $\phi=\pi$. Other parameters are $E_F=37.55$ and $\omega=0.002$.

shown in Fig. 6. At $\theta=0$, we see that the pumped current is sharply peaked at resonant energy. The pumped current is positive for $\phi=\pi/2$ and negative for $\phi=0$ and π. At $\theta=\pi/2$ or π, the pumped current at $\phi=\pi/2$ (dashed line) is much larger than that at other angles (not shown). Figure 7 displays the pumped current as a function of θ near resonant energy. For $\phi=\pi/2$ (dotted line), we see the usual behavior that large pumped current occurs at $\theta=0$ and it decreases to the minimum at $\theta=\pi$. For $\phi=0$ or π, however, we see completely different behavior. The pumped current is the still the largest at $\theta=0$ but the direction of the pumped current is reversed. As one increases θ, the pumped current decreases and reaches a flat region with almost zero pumped current. Now we study the effect of frequency to the pumped current versus θ [see Fig. 8(a)]. We will fix the phase difference to be $\phi=\pi/2$ with energy near resonance. At small frequency $\omega=0.002$ (dashed line), the pumped current versus θ shows usual behavior. When the frequency is increased to $\omega=0.004$ (dot-dashed line), two peaks show up symmetrically near $\theta=\pm\pi/4$ while the minimum is still at $\theta=\pi$. As frequency is increased further to $\omega=0.006$ (dotted line), the pumped current near $\theta=0$ reverses the direction and the new peak position shifts to $\theta\sim0.35\pi$. Upon further increasing ω, the curve of pumped current versus θ develops a flat region between $\theta=\pm0.35\pi$ with positive current, while the magnitude of the negative pumped current at $\theta=0$ becomes larger

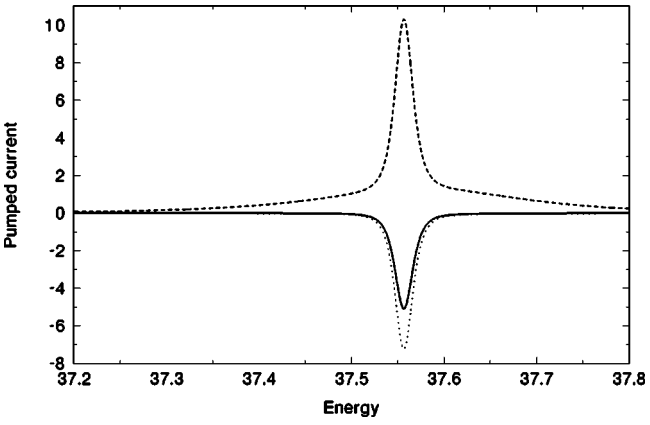

FIG. 6. The pumped current as a function of Fermi energy at finite frequency at $\theta=0$: Dotted line: $\phi=0$, dashed line: $\phi=\pi/2$, and solid line: $\phi=\pi$. Here $\omega=0.002$.

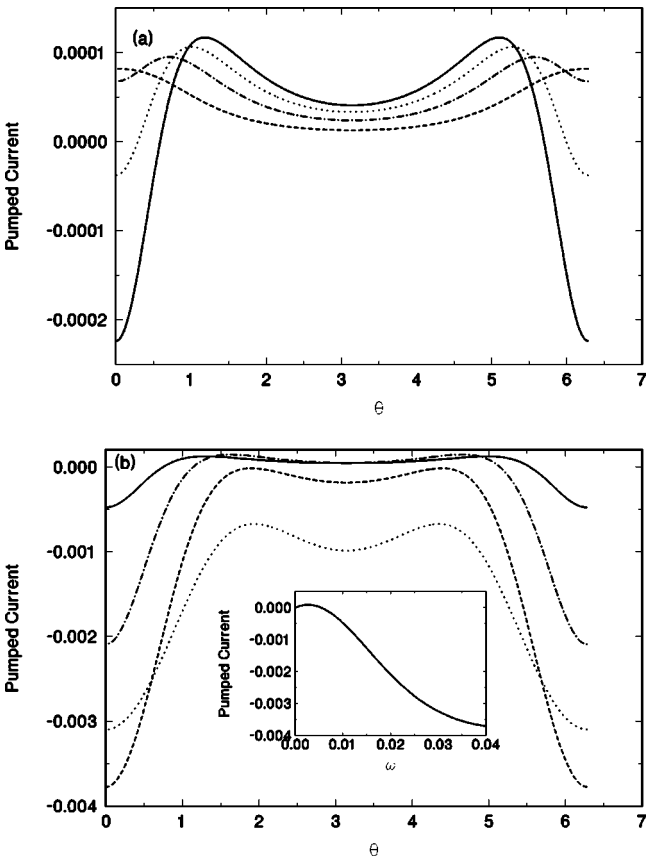

FIG. 8. The pumped current as a function of θ at different frequencies. (a) $\omega=0.002$ (short dashed line), 0.004 (dot-dashed line), 0.006 (dotted line), and 0.008 (solid line). (b) $\omega=0.01$ (solid line), 0.02 (dot-dashed line), 0.05 (short dashed line), and 0.1 (dotted line). Other parameters are $E_F=37.55$ and $\phi=\pi/2$. Inset: the pumped current as a function of frequency. Here $\theta=0$, $\phi=\pi/2$, and $E_F=37.55$.

[see Fig. 8(b)]. Finally, at even larger frequency $\omega=0.1$, all the pumped currents are negative. This behavior can be understood from the photon-assisted process.[19] The quantum interference between contributions due to photon emission (or absorption) near two pumping potentials is essential to understand the nature of pumped current. In addition to the interference effect, the pumped current is also affected by a competition between the photon emission and absorption processes which tend to cancel each other. It is the interplay between this competition and interference that gives rise to the interesting spin-valve effect for the pumped current. In the inset of Fig. 8(b), we show the pumped current versus pumping frequency at $\theta=0$. We see that at small frequency the current is positive and small, and at large frequency the current is much larger and is negative.

In summary, we have extended the previous parametric electron pumping theory to include the spin-polarized pumping effect. Our theory is based on the nonequilibrium Green's-function method, is valid for multimodes (in two or three dimensions), and can be easily extended to the case of multiprobes (although most of calculations are for two probes). In the parametric pumping, two kinds of driving forces are present: multiple pumping potentials inside the scattering system as well as the external bias in the multiprobes. Two cases are considered. In the adiabatic regime, the system is near equilibrium. In this case our theory is for general pumping amplitude. At finite frequency, the system is away from equilibrium. Our theory is up the quadratic order in pumping amplitude. This theory allows us to examine the pumped current in broader parameter space including pumping amplitude, pumping frequency, phase difference between two pumping potentials, and the angle between magnetization of two leads. From our numerical calculation, the spin-valve effect is clearly seen and the pumped current can be modulated by the angle θ.

ACKNOWLEDGMENTS

We gratefully acknowledge support of a RGC grant from the SAR Government of Hong Kong under Grant No. HKU 7091/01P and a CRCG grant from the University of Hong Kong.

APPENDIX

Now we show that

$$B\equiv\frac{1}{\tau}\int_0^\tau dt\int_{-\infty}^{t}dt_1\mathrm{Tr}[\mathbf{F}_0(t_1,t)\mathbf{G}(t,t_1)]$$
$$=\frac{V_\alpha V_\beta}{4}\int\frac{dE}{2\pi}\mathrm{Tr}\{\mathbf{F}_0(E)\mathbf{F}_1(E)[\mathbf{F}_2(E_+)e^{i\Delta_{\beta\alpha}}+e^{-i\Delta_{\beta\alpha}}\mathbf{F}_2(E_-)]\mathbf{F}_3(E)\},\tag{A1}$$

where

$$\mathbf{G}\equiv\mathbf{F}_1\mathbf{V}_\alpha\mathbf{F}_2\mathbf{V}_\beta\mathbf{F}_3\tag{A2}$$

and F_i's $(i=0,1,2,3)$ satisfy $F_i(t_1,t_2)=F_i(t_1-t_2)$.

Taking the Fourier transform

$$\mathbf{F}(t)=\frac{1}{2\pi}\int dEe^{-iEt}\mathbf{F}(E)\tag{A3}$$

we obtain

$$B=\frac{1}{\tau}\int_0^\tau dt\int_{-\infty}^{t}dt_1\int\frac{dE}{2\pi}\mathbf{F}_0(E)e^{-iE(t_1-t)}\int dxdy$$
$$\times[\mathbf{F}_1(t-x)V_\alpha(x)\mathbf{F}_2(x-y)V_\beta(y)\mathbf{F}_3(y-t_1)]$$
$$=\frac{1}{\tau}\int_0^\tau dt\int\prod_{i=1,5}\frac{dE_i}{2\pi}\int\frac{dE}{2\pi}\int_{-\infty}^{t}dt_1\int dxdy$$
$$\times\mathbf{F}_0(E)\mathbf{F}_1(E_1)\mathbf{V}_\alpha(E_2)\mathbf{F}_2(E_3)\mathbf{V}_\beta(E_4)\mathbf{F}_3(E_5)$$
$$\times e^{i(E-E_1)t}e^{i(E_5-E)t_1}e^{i(E_1-E_2-E_3)x}e^{i(E_3-E_4-E_5)y},$$

where

$$\mathbf{V}_\alpha(E)=\pi V_\alpha[e^{i\phi_\alpha}\delta(E_+)+e^{-i\phi_\alpha}\delta(E_-)].\tag{A4}$$

Integrating over x and y yields

$$B=\frac{1}{\tau}\int_0^\tau dt\int\prod_{i=1,5}\frac{dE_i}{2\pi}\int\frac{dE}{2\pi}\int_{-\infty}^{t}dt_1\mathbf{F}_0(E)$$
$$\times\mathbf{F}_1(E_1)\mathbf{V}_\alpha(E_2)\mathbf{F}_2(E_3)\mathbf{V}_\beta(E_4)\mathbf{F}_3(E_5)$$
$$\times e^{i(E-E_1)t}e^{i(E_5-E)t_1}(2\pi)^2\delta(E_1-E_2-E_3)$$
$$\times\delta(E_5-E_4-E_5).$$

Integrating over t_1,t and using Eq. (A4), we have

$$B=\int\frac{dE_2}{2\pi}\frac{dE_4}{2\pi}\frac{dE_5}{2\pi}\int\frac{dE}{2\pi}\frac{\mathbf{F}_0(E)}{i[E_5-E-i\delta]}\mathbf{F}_1(E_2+E_4+E_5)\mathbf{V}_\alpha(E_2)\mathbf{F}_2(E_4+E_5)\mathbf{V}_\beta(E_4)\mathbf{F}_3(E_5)\delta(E_2+E_4)$$
$$=\frac{V_\alpha V_\beta}{4}\int\frac{dE_5}{2\pi}\frac{dE}{2\pi}\frac{\mathbf{F}_0(E)}{i[E_5-E-i\delta]}\mathbf{F}_1(E_5)[\mathbf{F}_2(E_5+\omega)e^{i\Delta_{\beta\alpha}}+e^{-i\Delta_{\beta\alpha}}\mathbf{F}_2(E_5-\omega)]\mathbf{F}_3(E_5).$$

Now we look at Eq. (33), where there are two cases: (i) $\mathbf{F}_0=\boldsymbol{\Sigma}^a$ and $\mathbf{G}=\mathbf{G}_{11}^{(2)<}$ [see Eqs. (A2) and (36)] and (ii) $\mathbf{F}_0=\boldsymbol{\Sigma}^<$ and $\mathbf{G}=\mathbf{G}_{11}^{(2)r}$. In case (i) since $\mathbf{F}_0$ is analytic in the lower half plane, we use the theorem of residue to obtain

$$\int dE\frac{\mathbf{F}_0(E)}{i[E_5-E-i\delta]}=2\pi\mathbf{F}_0(E_5)\tag{A5}$$

and we thus obtain Eq. (A1). For case (ii) $\mathbf{G}$ is analytic in the upper half plane, we have

$$\int dE_5\frac{\mathbf{G}(E_5)}{i[E_5-E-i\delta]}=2\pi\mathbf{G}(E),\tag{A6}$$

so Eq. (A1) remains.

*Electronic address: jianwang@hkusub.hku.hk
[1] P.W. Brouwer, Phys. Rev. B **58**, R10 135 (1998).
[2] I.L. Aleiner and A.V. Andreev, Phys. Rev. Lett. **81**, 1286 (1998).
[3] M. Switkes, C. Marcus, K. Capman, and A.C. Gossard, Science **283**, 1905 (1999).
[4] F. Zhou, B. Spivak, and B.L. Altshuler, Phys. Rev. Lett. **82**, 608 (1999).
[5] T.A. Shutenko, I.L. Aleiner, and B.L. Altshuler, Phys. Rev. B **61**, 10 366 (2000).
[6] Y.D. Wei, J. Wang, and H. Guo, Phys. Rev. B **62**, 9947 (2000).
[7] I.L. Aleiner, B.L. Altshuler, and A. Kamenev, Phys. Rev. B **62**, 10 373 (2000).
[8] J.E. Avron, A. Elgart, G.M. Graf, and L. Sadun, Phys. Rev. B **62**, R10 618 (2000).
[9] Y. Levinson, O. Entin-Wohlman, and P. Wolfle, Physica A **302**, 335 (2001).
[10] P.W. Brouwer, Phys. Rev. B **63**, 121303 (2001); M.L. Polianski and P.W. Brouwer, *ibid.* **64**, 075304 (2001).
[11] M. Moskalets and M. Buttiker, Phys. Rev. B **64**, 201305 (2001).
[12] J.E. Avron, A. Elgart, G.M. Graf, and L. Sadun, Phys. Rev. Lett. **87**, 236601 (2001).
[13] J. Wang *et al.*, Appl. Phys. Lett. **79**, 3977 (2001).
[14] M.G. Vavilov, V. Ambegaokar, and I.L. Aleiner, Phys. Rev. B **63**, 195313 (2001).
[15] Y.D. Wei, J. Wang, H. Guo, and C. Roland, Phys. Rev. B **64**, 115321 (2001).
[16] F. Renzoni and T. Brandes, Phys. Rev. B **64**, 245301 (2001).
[17] Y. Makhlin and A.D. Mirlin, Phys. Rev. Lett. **87**, 276803 (2001).
[18] C.S. Tang and C.S. Chu, Solid State Commun. **120**, 353 (2001).
[19] B.G. Wang, J. Wang, and H. Guo, Phys. Rev. B **65**, 073306 (2002).
[20] J. Wang and B.G. Wang, Phys. Rev. B **65**, 153311 (2002).
[21] Y. Levinson, O. Entin-Wohlman, and P. Wolfle, cond-mat/0104408 (unpublished).
[22] O. Entin-Wohlman, A. Aharony, and Y. Levinson, Phys. Rev. B **65**, 195411 (2002).
[23] M. Moskalets and M. Buttiker, Phys. Rev. B **66**, 035306 (2002).
[24] M.L. Polianski, M.G. Vavilov, and P.W. Brouwer, Phys. Rev. B **65**, 245314 (2002).
[25] O. Entin-Wolman and A. Aharony, Phys. Rev. B **66**, 035329 (2002).
[26] B.G. Wang and J. Wang, Phys. Rev. B **65**, 233315 (2002).
[27] B.G. Wang and J. Wang, Phys. Rev. B **66**, 125310 (2002).
[28] M. Blaauboer, Phys. Rev. B **65**, 235318 (2002).
[29] E.R. Mucciolo *et al.*, cond-mat/0112157 (unpublished).
[30] J.L. Wu, B.G. Wang, and J. Wang (unpublished).
[31] R. Meservey and P.M. Tedrow, Phys. Rep. **238**, 173 (1994); M. Baibich *et al.*, Phys. Rev. Lett. **61**, 2472 (1988); G.A. Prinz, Science **282**, 1660 (1998); D.J. Monsma, J.C. Lodder, Th.J.A. Popma, and B. Dieny, Phys. Rev. Lett. **74**, 5260 (1995); D.J. Monsma, R. Vlutters, and J.C. Lodder, Science **281**, 407 (1998); A. Wolf *et al.*, *ibid.* **294**, 1488 (2001).
[32] J.C. Slonczewski, Phys. Rev. B **39**, 6995 (1989).
[33] J.S. Moodera, L.R. Kinder, T.M. Wong, and R. Meservey, Phys. Rev. Lett. **74**, 3273 (1995); S. Zhang, P.M. Levy, A.C. Marley, and S.S.P. Parkin, *ibid.* **79**, 3744 (1997); X.D. Zhang, B.Z. Li, G. Sun, and F.C. Pu, Phys. Rev. B **56**, 5484 (1997); J.S. Moodera, J. Nowak, and R.J.M. van de Veerdonk, Phys. Rev. Lett. **80**, 2941 (1998); J. Barnaś and A. Fert, *ibid.* **80**, 1058 (1998); L. Sheng, Y. Chen, H.Y. Teng, and C.S. Ting, Phys. Rev. B **59**, 480 (1999); K. Tsukagoshi, B.W. Alphenaar, and H. Ago, Nature (London) **401**, 572 (1999); H. Mehrez *et al.*, Phys. Rev. Lett. **84**, 2682 (2000); N. Sergueev *et al.*, Phys. Rev. B **65**, 165303 (2002).
[34] N.N. Bogoliubov, J. Phys. (Moscow) **11**, 23 (1947).
[35] B.G. Wang, J. Wang, and H. Guo, J. Phys. Soc. Jpn. **70**, 2645 (2001).
[36] M.P. Anantram and S. Datta, Phys. Rev. B **51**, 7632 (1995).
[37] A.P. Jauho, N.S. Wingreen, and Y. Meir, Phys. Rev. B **50**, 5528 (1994).
[38] B.G. Wang, J. Wang, and H. Guo, Phys. Rev. Lett. **82**, 398 (1999); J. Appl. Phys. **86**, 5094 (1999).
[39] C.A. Stafford and N.S. Wingreen, Phys. Rev. Lett. **76**, 1916 (1996); Q.F. Sun, J. Wang, and T.H. Lin, Phys. Rev. B **58**, 13 007 (1998); *ibid.* **59**, 13 126 (1999); *ibid.* **61**, 12 643 (2000); H.K. Zhao and J. Wang, Eur. Phys. J. B **9**, 513 (1999).
[40] M. Büttiker, J. Phys.: Condens. Matter **5**, 9361 (1993).
[41] T. Gramespacher and M. Büttiker, Phys. Rev. B **56**, 13 026 (1997).
[42] For the system of Fe/Ge/Fe with $a=100A$, the energy unit is $E=4.64$ meV which corresponds to frequency $\omega=1.1\times10^{12}$ Hz. The unit of the pumped current in the adiabatic regime depends on the pumping frequency ω. If $\omega=100$ MHz, then the pumped current is 1.6×10^{-11} A. For pumped current at finite frequency, the unit of current is 2×10^{-6} A.
[43] M.K. Yip, J. Wang, and H. Guo, Z. Phys. B: Condens. Matter **104**, 463 (1997).